Motion of 'hopping' particles in a constant force field

1985 J. Phys. A: Math. Gen. 18 2583

(http://iopscience.iop.org/0305-4470/18/13/033)

J. Phys. A: Math. Gen. 18 (1985) 2583-2589. Printed in Great Britain

Motion of 'hopping' particles in a constant force field

Jean-Pierre Gallinar† and Daniel C Mattis
Department of Physics, University of Utah, Salt Lake City, Utah 84112, USA

Received 21 November 1984

Abstract. We study the eigenstates of electrons or holes constrained to 'hop' from site to neighbouring site on a lattice ('Wannier particles'), when they are subjected to strong fields of constant force. Principal applications are to inversion layers at the surface of semiconductors. It is seen that the exact solutions differ considerably from those found in the continuum 'effective-mass' approximation. We also analyse the eigenstates of *two* Wannier particles when the only force is their mutual attraction of constant force.

1. Introduction

Recently, Gallinar (1984) obtained the formal solution for the eigenvalue spectrum of Schrödinger's equation for a particle 'hopping' on a Bethe lattice (henceforth to be denoted, for brevity, a 'Wannier particle') under the influence of an arbitrary potential of spherical symmetry, of which the Coulomb problem is a special case. In the present work we present the explicit solution for Wannier particles subject to linear or piecewise linear potentials. Applications include electrons or holes in inversion layers near the surface of a semiconductor, and the variously defined particles of lattice gauge theories (see review by Kogut 1979).

In the case of electrons or holes in solids, particles in Wannier states about a given site have a known matrix element for transfer to neighbouring sites, one which can be computed with knowledge of the band structure. As particles in Bloch states within each band are commonly denoted 'Bloch particles', it is natural that we denote electrons or holes in the localised representation of Wannier states of a given band, 'Wannier particles'. We shall make the further approximation, that the 'hopping' matrix elements connect only nearest-neighbour sites in 'cubium' (the linear chain, simple quadratic, or simple cubic lattices). In our calculations, within the limitations of this idealised model, we shall strive for exact results, to see in what way the solutions of the discrete models differ from the 'continuum' or 'effective mass' approximations. If the surface fields restrict particles to within one or two layers from the surface of a semiconductor, it seems absurd to calculate their properties using a continuum (i.e. long-wavelength) approximation, yet that is precisely what one has been forced to do in the absence of solutions of the type we shall obtain in these pages.

Assuming we can factor the wavefunctions in the direction perpendicular to the surface (x) from the functions relating to motion within planes parallel to the surface (y, z), and that the potential is applied perpendicular to the surface, the relevant part

† On sabbatical leave from Departamento de Física, Universidad Simón Bolívar, Apartado 80659, Caracas 108, Venezuela (present address).

0305-4470/85/132583+07$02.25

of the three-dimensional problem reduces to that of a particle on a linear chain, with x discrete ($x = na$, a = distance between planes and n = integer). The solutions odd in x automatically satisfy the 'hard wall' boundary condition at $n = 0$. For completeness, however, we also give the even solutions. (Both parities enter into the problem of two particles subject to a mutual attraction of constant force.)

Such one-dimensional problems can generally be solved by means of a continued fraction representation of the relevant Green functions (Hubbard 1979). This powerful method enables one to obtain the eigenvalue spectrum of an arbitrary Hamiltonian of the form,

$$H = -\sum C_n\{|n+1\rangle\langle n| + |n-1\rangle\langle n|\} + \sum U_n|n\rangle\langle n|. \tag{1}$$

Indeed, we have used the Green function continued-fraction solution of the linear-potential problem to verify the essential conclusions *which we shall now derive by simpler means.* For, in the special case of a linear potential and an homogeneous band structure (C_n = constant), it happens that judicious comparison of Schrödinger's equation with the well known difference equations of Bessel functions yields the desired solutions, without further ado. It is rare to find instances in the physics of discrete lattices where a non-trivial problem receives such a simple, direct, and complete solution, and we present this research for its intrinsic interest, as well as for its applications to semiconductor physics. (Indeed, aside from two other examples, (1) the aforementioned lattice Coulomb problem, and (2) the parabolic potential $U = 1/2Kn^2$ (for which a suitable version of Mathieu's equation yields the complete solutions) our problem may provide a uniquely exactly soluble example in lattice physics.)

2. Eigenvalues and eigenfunctions

With the choices

$$C_n = C(\text{constant}) \text{ and } U_n = \mathcal{F}|n| \; (\mathcal{F} = q\boldsymbol{E}a) \tag{2}$$

the Hamiltonian in (1) describes a particle hopping with constant matrix element C from site to site on a linear chain, in a potential proportional to the applied field $\boldsymbol{E}$, charge q, and site index n. It must be assumed that the product $q\boldsymbol{E} > 0$, or else the states of lowest energy will be at ∞. The Hamiltonian is explicitly even about $n = 0$, thus its eigenstates have even or odd parity. One of the effects of placing an infinitely high barrier at the surface at $n = 0$ is to single out the *odd parity* eigenstates of our Hamiltonian, for they spontaneously satisfy the boundary condition $\Psi(n = 0) = 0$. The potential U_n at $n > 0$ serves to confine carriers to the neighbourhood of the surface. All the states we find are *bound states.* For completeness, we also consider the *even parity* bound states (which, however, satisfy not the aforementioned boundary condition, but another which we shall shortly derive).

Consider an arbitrary, normalised eigenstate in the form,

$$\Psi = \sum A_n|n\rangle, \qquad \text{with } \sum |A_n|^2 = 1. \tag{3}$$

The Schrödinger equation $H\Psi = E\Psi$ will yield an equation for the coefficients, which with the choices (2) takes on the aspect:

$$A_{n+1} + A_{n-1} = (\mathcal{F}|n| - E)(C^{-1})A_n. \tag{4}$$

For the solution to be well behaved, the coefficients must vanish sufficiently fast at $n=\infty$. Both types of Bessel functions, J_n (first kind) and Y_n (second kind), satisfy difference equations similar to (4). Credit for first recognising this is due Merrifield (1963). This author, however, did not appreciate the importance of the boundary conditions at $n=0$ (and therefore obtained unphysical results). Of the two types of Bessel functions, Y_n diverges at large $|n|$ and is thus unsuited to the present applications, while J_n vanishes asymptotically sufficiently fast to be normalised and is thus an excellent candidate for identifying with A_n. The appropriate equation for Bessel's functions (Abramowitz and Stegun 1965) is

$$J_{\nu+1}(Z)+J_{\nu-1}(Z)=(2\nu/Z)J_\nu(Z). \tag{5}$$

Thus, comparison of (5) with (4) at all $n\neq 0$ yields

$$A_n=DJ_\nu(Z), \tag{6}$$

where D is the normalisation constant. Defining the energy eigenvalue in dimensionless units, $w=E/\mathcal{F}$, and the parameter $Z=2C/\mathcal{F}$, we observe that the identification (6) requires

$$\nu=|n|-w. \tag{7}$$

We now distinguish the two cases. For odd parity, $A_0=0$ requires

$$J_{-w}(Z)=0 \qquad \text{odd parity.} \tag{8}$$

The solution of (8) yields all the eigenvalues of the inversion-layer problem (where the surface barrier at $n=0$ forces all A_n for $n\leqslant 0$ to vanish). Fixing Z, the solutions are found as functions of w (in the range $\infty > w > -2C/\mathcal{F}$).

We now turn to the even parity states. The requirement that equations (4) and (5) agree at $n=0$, with $A_{-1}=A_1$, easily translates into $J_{-1-w}(Z)=J_{1-w}(Z)$. Hence by another well known identity of Bessel functions (Abramowitz and Stegun 1965), i.e.

$$J_{\nu+1}(Z)-J_{\nu-1}(Z)=2(\mathrm{d}/\mathrm{d}Z)J_\nu(Z) \tag{9}$$

we obtain a more 'transparent' boundary condition:

$$(\mathrm{d}/\mathrm{d}Z)J_{-w}(Z)=0 \qquad \text{even parity} \tag{10}$$

to be evaluated at $Z=2C/\mathcal{F}$. Those values of w in the range $w>-2C/\mathcal{F}$ for which (10) is obeyed will constitute the even-parity eigenvalue spectrum of H.

In figure 1 we show the lowest two even levels ($n=0, 1$) and odd levels (labelled $\tilde{n}=1, 2$) as a function of $\mathcal{F}$, and some comparison with the continuum approximation. (The continuum theory is solved in the appendix.) Figure 2 provides a microscopic examination of the strong-coupling region of figure 1. We see that while the individual energy levels of the Wannier particles maintain their identities and separations, the curves corresponding to the continuum theory all merge at the origin.

Possibly, either dielectric breakdown, or tunnelling from one conduction band to the next, will characterise the strong-coupling regime physically. However, these are phenomena which cannot be examined within the framework of the Hamiltonian (1). What *is* clear, is that continuum theory breaks down in strong electric fields, and the discreteness of the lattice *must* then be taken into account.

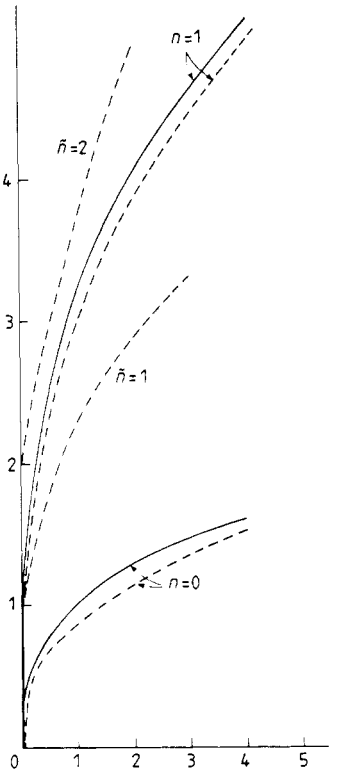

Figure 1. The broken curves are a plot of energy $w+2C/\mathcal{F}$ (vertical axis) against $C/\mathcal{F}$ (horizontal axis), where $C=\frac{1}{4}$ bandwidth and $\mathcal{F}$ measures the strength of the force field. The even parity levels are denoted n, the odd parity levels $\tilde{n}$. The $n=0,1$ even-parity energy levels in the continuum 'effective-mass' approximation are also shown for comparison. (The $\tilde{n}=1,2$ continuum curves are omitted for visual convenience, as they almost coincide with the exact solutions on the scale of this graph.)

3. Two-particle problem

With the one-body problem reduced to quadrature, we now consider a two-body problem defined as follows: one particle hops with matrix elements C between nearest-neighbour sites, while the second hops with matrix elements V. This simulates an electron in the conduction band (C) and a hole in the valence band (V), which are now assumed to attract with a constant force. In one dimension, this is equivalent to a potential $U_{n-m}=\mathcal{F}|n-m|$, where n is the coordinate of the C particle, and m that of the V particle. The energies are the eigenvalues of an Hamiltonian

$$H=-\sum\{C[|n+1,\,m\rangle\langle n,\,m|+|n-1,\,m\rangle\langle n,\,m|] + V[|n,\,m+1\rangle\langle n,\,m|+|n,\,m-1\rangle\langle n,\,m|]\}+\sum U_{n-m}|n,\,m\rangle\langle n,\,m|. \tag{11}$$

If either C or V is zero, we recover the one-particle solutions explicitly. The same can be seen to be true when both are non-zero (after some manipulation). Denoting the two-particle eigenstates Ψ, with

$$\Psi=\sum B(n,\,m)|n,\,m\rangle, \tag{12}$$

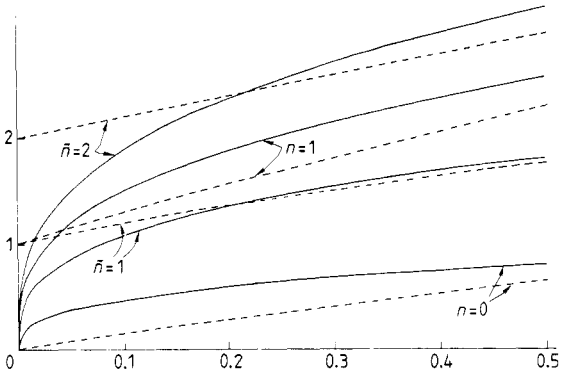

Figure 2. Enlargement of figure 1 in the strong-coupling region, showing the two lowest even- and odd-parity levels in the discrete (broken curves) and in the continuum (full curves) theories. The discrepancies are obvious when the potential energy change per hop is comparable to the hopping matrix element (bandwidth parameter).

we write $B(n, m)$ in the form

$$B(n, m) = \{\exp i[\tfrac{1}{2}ka(n+m)+(n-m)\phi]\}A(n-m) \tag{13}$$

where k is the wavevector associated with centre-of-mass motion, while ϕ is an as yet undetermined parameter. After simple algebra, we obtain the equation satisfied by $A(p)$:

$$A(p+1)+A(p-1) = (\mathcal{F}|p|-E)(e(k))^{-1}A(p) \tag{14}$$

with $e(k)$ a positive quantity given by

$$e(k) = [V^2+C^2+2VC\cos(ka)]^{1/2} \tag{15}$$

and $\phi = \phi(k)$ chosen as follows:

$$\phi(k) = \tan^{-1}\{[(C-V)/(C+V)]\tan(ka/2)\}. \tag{16}$$

Apart from multiplicative normalisation constants, the even and odd parity solutions of Schrödinger's equation are

$$A(p) = J_{|p|-w}(Z) \qquad \text{even} \tag{17a}$$

and

$$A(p) = (\operatorname{sgn} p)J_{|p|-w}(Z) \qquad \text{odd} \tag{17b}$$

subject to the respective boundary (i.e., eigenvalue) conditions,

$$(\mathrm{d}/\mathrm{d}Z)J_{-w}(Z) = 0 \qquad \text{even} \tag{18a}$$

and

$$J_{-w}(Z) = 0 \qquad \text{odd} \tag{18b}$$

evaluated at $Z = 2e(k)/\mathcal{F}$. The resulting eigenvalues $w = E/\mathcal{F}$ determine the energies E. Figure 3 displays some of the solutions, for the special case $V = C$. Each of the discrete one-particle states is now spread into a band, denoted $E_n(k)$. Because these bands become increasingly narrow as the quantum number n is increased, we can

expect that the 'effective mass' of the composite particle increases with quantum number, as shown in the appendix. Now, although the question of the dependence of mass on internal interactions has previously been solved in all generality, for an exciton subject to arbitrary central forces (Mattis and Gallinar 1984), yet the particular problem at hand (where *all* the states are bound) does merit a separate analysis, given in the appendix.

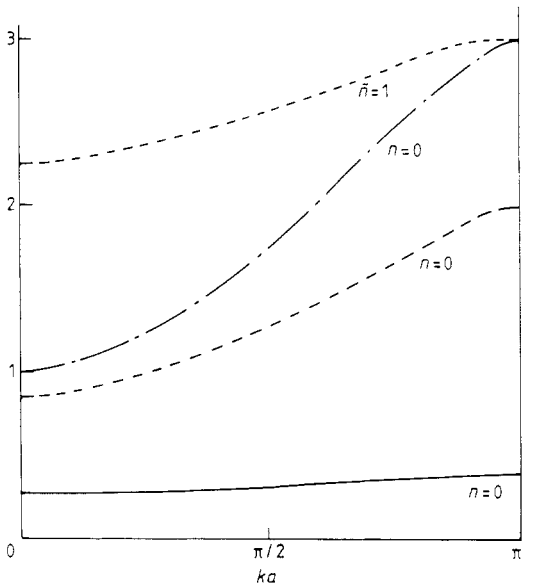

Figure 3. Plot of $(E_n(k)+4C)/\mathcal{F}$ against crystal momentum ka for two identical ($V=C$) particles bound by a mutual potential of constant force, for $n=0$ and $\tilde{n}=1$ at different values of $1/f=C/\mathcal{F}$. The continuous curve corresponds to $1/f=0.1$ and is almost flat. The two broken curves are at $1/f=0.5$, while the chain curve has $1/f=0.75$. (Note that the $\tilde{n}=1$ band is narrower than $n=0$, indicating that the total mass of the composite particle increases with quantum number—a trend proved in the appendix.)

Acknowledgments

The authors wish to thank Marek Karliner at SLAC for obtaining some preliminary solutions of equation (8) for us, using the computer language 'Speakeasy'. One of us (J-PG) has been a visiting scholar at the University of Utah, during which time he was the beneficiary of Grant No S1-1207 awarded by the Consejo Nacional de Investigaciones Científicas y Tecnológicas (CONICIT), Venezuela. The support of this research by the National Science Foundation, Grant No DMR-81-06223 is also gratefully acknowledged.

Appendix

We treat the continuum limit ($a\to 0$ with C, $V\to\infty$, such that Va^2 and Ca^2 are both finite). The eigenvalues of the resulting Schrödinger equation are straightforwardly

$$E_n(k)=(1/2)(m_1+m_2)^{-1}\hbar^2k^2+z_n(\hbar^2q^2E^2/2\mu)^{1/3} \tag{A1}$$

where μ is the reduced mass m_1m_2/m_1+m_2, z_n is the nth root of $\mathrm{Ai}(-z)=0$ (odd) or $\mathrm{Ai}'(-z)=0$ (even), and $\mathrm{Ai}(z)$ is the well known Airy function (Watson 1944). We have made use of this in calculating the plotted curves.

The calculation of the true effective mass of the 'Wannier exciton', $M_n^* \neq m_1+m_2$, is more involved. Here we shall give a mere summary of our extensive calculations, indicating that the exciton bands become narrower as their quantum number increases. We use a result (Watson 1944) for $J_\nu(z)=0$, i.e.

$$\frac{\mathrm{d}z}{\mathrm{d}\nu}=2z\int_0^\infty K_0(2z\sinh t)\,\mathrm{e}^{-2\nu t}\,\mathrm{d}t \tag{A2}$$

where $K_0(x)$ is the modified Bessel function of zero order and second kind. The definition of M_n^* is $\hbar^2/\partial^2E_n(k)/\partial k^2|_{k=0}$ and, after manipulations, it becomes:

$$M_n^*=\frac{2\hbar^2(V+C)^2}{VCa^2\mathscr{F}}\int_0^\infty K_0\frac{4(V+C)\sinh t}{\mathscr{F}}\exp(b_nt)\,\mathrm{d}t \tag{A3}$$

where $b_n=2[E_n(0)-2(V+C)]\mathscr{F}$ increases with $E_n(0)$. As the latter diverges as $n\to\infty$, so will M_n^*.

In the rest of this appendix, we show how to obtain the 'effective-mass' approximation (EMA) for some of our results. We first show how to obtain (A1). As proved in the text, the odd spectrum for $E_n(k)$ is given by the roots of $J_{-w}(Z)=0$, where $Z=2e(k)/\mathscr{F}$ and $w=E_n/\mathscr{F}$, while the even spectrum is given by the roots of $\mathrm{d}/\mathrm{d}ZJ_{-w}(Z)=0$. For the sake of reference, we shall work with the odd spectrum condition. To compare with the continuum limit, we must add the energy $2(V+C)$ to $E_n(k)$, as has also been done in figures 1-3. We expand $e(k)$ to obtain

$$e(k)\cong(V+C)-\frac{VCk^2a^2}{2(V+C)}+\mathrm{O}(k^4). \tag{A4}$$

The equation $J_{-w}(Z)=0$ then gives equivalently that

$$J_\nu\left(\frac{2(V+C)a^2}{\mathscr{F}a^2}-\frac{VCk^2a^2}{\mathscr{F}(V+C)}\right)=0 \tag{A5}$$

with

$$\nu\equiv-\frac{E_n(k)}{\mathscr{F}}+\frac{2(V+C)a^2}{\mathscr{F}a^2}. \tag{A6}$$

In the EMA limit, (A5) implies

$$\lim_{\nu\to\infty}J_\nu\left(\nu+\frac{E_n(k)}{\mathscr{F}}-\frac{VCk^2a^2}{\mathscr{F}(V+C)}\right)=0. \tag{A7}$$

When $a\to0$, we obtain from (A6) that

$$a\cong(\hbar^2/qE\mu\nu)^{1/3}$$

and substitution of this into (A7) gives

$$\lim_{\nu\to\infty}J_\nu\left[\nu+\left(E_n(k)-\frac{VCk^2a^2}{V+C}\right)(\mu\nu/\hbar^2q^2E^2)^{1/3}\right]=0. \tag{A8}$$

By now using the limit (Abramowitz and Stegun 1965)

$$\lim_{\nu\to\infty}J_\nu(\nu+\lambda\nu^{1/3})=(2/\nu)^{1/3}\mathrm{Ai}(-2^{1/3}\lambda)+\mathrm{O}(\nu^{-1}) \tag{A9}$$

the equation (A8) leads finally to the EMA limit (A1), with the natural identifications $Va^2 = \hbar^2/2m_1$ and $Ca^2 = \hbar^2/2m_2$. *Mutatis mutandis*, one can also obtain analogous relationships for the even spectrum, leading to (A1) too.

Finally, it is straightforward to show that the appropriate EMA limit for M_n^*, namely, $M_n^* = m_1 + m_2$, may be obtained from (A3) by using the logarithmic representation for $\sinh^{-1} t$. After a change of variables and some manipulations, one obtains from (A3), that

$$\lim_{a\to 0} M_n^* = \frac{\hbar^2(V+C)I}{2VCa^2} = m_1 + m_2 \tag{A10}$$

since

$$I = \int_0^\infty \mathrm{d}y K_0(y)\, \mathrm{e}^{-y} = 1.$$

References

Abramowitz M and Stegun I A 1965 *Handbook of Mathematical Functions* (New York: Dover)
Gallinar J-P 1984 *Phys. Lett.* **103A** 72
Hubbard J 1979 *Phys. Rev.* B **19** 1828
Kogut J 1979 *Rev. Mod. Phys.* **51** 659
Mattis D C and Gallinar J-P 1984 *Phys. Rev. Lett.* **53** 1391
Merrifield R E 1963 *J. Chem. Phys.* **39** 3540
Watson G N 1944 *A Treatise on the Theory of Bessel Functions* (Cambridge: CUP)